Contribution No. 7549 from the Arthur Amos Noyes Laboratory, California Institute of Technology, Pasadena, California 91125, and Contribution from the Department of Chemistry, University of California, Los Angeles, California 90024

X-ray Crystallographic and Solution NMR Structural Studies of Binuclear Rhodium and Iridium Isocyanide Complexes

Andrew W. Maverick,[1a] Terrance P. Smith,[1a] Emily F. Maverick,[1b] and Harry B. Gray*[1a]

Received February 4, 1987

The structures of two $M_2(TMB)_4^{4+}$ complexes (TMB = 2,5-diisocyano-2,5-dimethylhexane; M = Rh, Ir) have been determined by X-ray crystallography. $[Rh_2(TMB)_4Cl_2](PF_6)_2$: orthorhombic, space group *Pbcn* (No. 60); a = 13.846 (5), b = 24.773 (3), c = 17.068 (4) Å; Z = 4; R = 0.075 for 1405 reflections with $F_o > 3\sigma(F)$. $[Ir_2(TMB)_4I_2](BPh_4)_2 \cdot 1.5(CH_3)_2CO$: orthorhombic, space group *Pccn* (No. 56); a = 15.141 (8), b = 28.104 (14), c = 23.877 (12) Å; Z = 4; R = 0.127 for 2839 reflections with $F_o > 3\sigma(F)$. The metal-metal distances in the two complexes are 2.770 (3) (Rh) and 2.803 (4) Å (Ir); C-M-M-C torsion angles are 33 (Rh) and 31° (Ir). Evidence for interconversion of Δ- and Λ-type enantiomers of these and related TMB complexes based on variable-temperature solution ^1H NMR data is presented. Barriers ΔG^* to the Δ-Λ inversion are between 50 and 62 kJ mol^{-1} for four different $M_2(TMB)_4^{z}$ complexes (M = Rh, Ir; z = 2+, 4+). This inversion or a related process with lower activation energy may be responsible for the relatively short $^3A_{2u}$ excited-state lifetime in $Rh_2(TMB)_4^{2+}$. These data, as well as crystallographic comparisons with a number of other polynuclear isocyanide complexes in the literature, suggest that the relative orientation of the $M(CN)_4$ moieties is determined principally by ligand conformation and only slightly by direct electronic interactions.

Introduction

Our recent studies of polynuclear complexes of isocyanides have concentrated on their spectroscopic and photochemical properties. Early reports concerned the oligomerization of planar mononuclear isocyanide complexes in solution[2,3] and the use of 1,3-diisocyanopropane ("bridge") as a bridging ligand for the specific synthesis of binuclear species.[4,5] Since then "bridge", 2,5-diisocyano-2,5-dimethylhexane (TMB), and *cis*-1-isocyano-4-(1-isocyano-1-methylethyl)-1-methylcyclohexane (1,8-diisocyano-*p*-menthane, or DMB) have been used to synthesize a variety of polynuclear complexes. We report here the crystal structures of two complexes of TMB, dynamic NMR data concerning the conformations of these and related ions in solution, and crystallographic comparisons with similar ions in the literature.

All of these ions have in common the M_2L_8 unit **1**. Our objective in carrying out the structural studies was to examine the

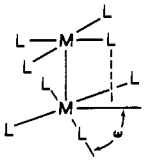

1

relationship between metal-metal distance and the angle ω as a function of L. For monodentate ligands L, ω and the metal-metal distance should be controlled primarily by electronic factors involving the metal atoms (and their immediate coordination environment) and by steric repulsions between ligands. In corresponding complexes $M_2(LL)_4$ of bidentate ligands LL, however, the ligand itself introduces additional steric constraints, and these may be responsible for changes in both photophysical properties and gross molecular structure. Thus, we wished to explore the interconnections between solid-state conformation and dynamic properties in solution, between the steric requirements of the ligands and the conformation at M, and between molecular rigidity and photophysics.

Experimental Section

Rhodium and Iridium Complexes. Manipulations involving $Ir_2(TMB)_4^{2+}$ were carried out in a drybox. $[Ir_2(TMB)_4](BPh_4)_2$ was prepared by mixing stoichiometric quantities of $[(\eta^4\text{-}1,5\text{-cyclooctadiene})IrCl]_2$[6] and TMB[7] in dichloromethane solution, dissolving the resulting deep turquoise solid in CH_3OH, and adding excess $NaBPh_4$. The crude product was purified by recrystallization from acetone. $[Rh_2(TMB)_4](PF_6)_2$[7] and $[Rh_2(TMB)_4](O_3SCF_3)_2$[8] were prepared by literature methods. $[Ir_2(TMB)_4I_2](BPh_4)_2$ was prepared by titration, using solutions of $[Ir_2(TMB)_4](BPh_4)_2$ and I_2 in CH_3CN. Removal of the solvent left a yellow solid. This was stirred with methanol and the resulting slurry filtered. Addition of methanolic $NaBPh_4$ to the filtrate gave a yellow precipitate that was combined with the yellow solid residue and crystallized from acetone. An analogous method was used to prepare $[Rh_2(TMB)_4Br_2](BPh_4)_2$.

Crystals of $[Ir_2(TMB)_4I_2](BPh_4)_2 \cdot x(CH_3)_2CO$ were grown by slow evaporation of an acetone solution. Crystals of $[Rh_2(TMB)_4Cl_2](PF_6)_2$, grown by cooling a hot acetonitrile-toluene solution, were supplied by Dr. Vincent M. Miskowski.

Table I. Crystallographic Data

formula	$C_{40}H_{64}Cl_2F_{12}N_8P_2Rh_2$	$C_{92.5}H_{113}I_2B_2N_8O_{1.5}Ir_2$
space group	*Pbcn* (No. 60)	*Pccn* (No. 56)
a/Å	13.846 (5)	15.141 (8)
b/Å	24.773 (3)	28.104 (14)
c/Å	17.068 (4)	23.877 (12)
$\alpha = \beta = \gamma$/deg	90.00 (2)	90.00 (4)
V/Å^3	5854	10160
Z	4	4
ρ_{calcd}/g cm^{-3}	1.39	1.32
color	yellow	yellow-brown
cryst habit	needle	rect parallelepiped
cryst dimens/mm^3	0.1 × 0.1 × 0.2	0.29 × 0.25 × 0.22
diffractometer	Enraf-Nonius CAD4	Syntex $P2_1$
monochromator	graphite	graphite
radiation (λ/Å)	Mo Kα (0.71069)	Mo Kα (0.71069)
T/K	~293	~295
abs coeff, μ/cm^{-1}	6.98	31.1
abs cor	no	yes, 0.39-0.69[a]
no. reflcns for cell param refinement	4 (each in 2 settings)	15
scan type	θ-2θ	θ-2θ
octant	$+h,+k,+l$	$+h,+k,+l$
2θ range	0° < 2θ < 48°	0° < 2θ < 50°
no. of indep reflcns measd	4573	9019
no. of reflcns used ($F_o > 3\sigma(F)$) ($N_{observns}$)	1405	2839
no. of params refined[b] (N_{params})	314	217
max peak height in final diff map/e Å^{-3}	1	3
R[c]	0.075	0.127
R_w[d]	0.073	0.085
goodness of fit[e]	1.87	2.60

[a] Transmission coefficients for absorption correction based on indexing of crystal faces. [b] The quantity refined was $w(|F_o| - |F_c|)^2$, where $w = 1/(\sigma(F_o))^2$ (σ estimated from counting statistics). [c] $R = \sum||F_o| - |F_c||/\sum|F_o|$. [d] $R_w = [\sum w(|F_o| - |F_c|)^2/\sum w|F_o|^2]^{1/2}$. [e] $S = [\sum w(|F_o| - |F_c|)^2/(N_{observns} - N_{params})]^{1/2}$.

(1) (a) California Institute of Technology. (b) University of California.
(2) Mann, K. R.; Gordon, J. G., II; Gray, H. B. *J. Am. Chem. Soc.* **1975**, *97*, 3553.
(3) Mann, K. R.; Lewis, N. S.; Williams, R. M.; Gray, H. B.; Gordon, J. G., II. *Inorg. Chem.* **1978**, *17*, 828.
(4) Lewis, N. S.; Mann, K. R.; Gordon, J. G., II; Gray, H. B. *J. Am. Chem. Soc.* **1976**, *98*, 7461.
(5) Mann, K. R.; Lewis, N. S.; Miskowski, V. M.; Erwin, D. K.; Hammond, G. S.; Gray, H. B. *J. Am. Chem. Soc.* **1977**, *99*, 5525.
(6) Winkhaus, G.; Singer, H. *Z. Naturforsch., B: Anorg. Chem., Org. Chem., Biochem., Biophys., Biol.* **1965**, *20B*, 602.
(7) Mann, K. R.; Thich, J. A.; Bell, R. A.; Coyle, C. L.; Gray, H. B. *Inorg. Chem.* **1980**, *19*, 2462.
(8) Sigal, I. S.; Gray, H. B. *J. Am. Chem. Soc.* **1981**, *103*, 2220.

0020-1669/87/1326-4336$01.50/0

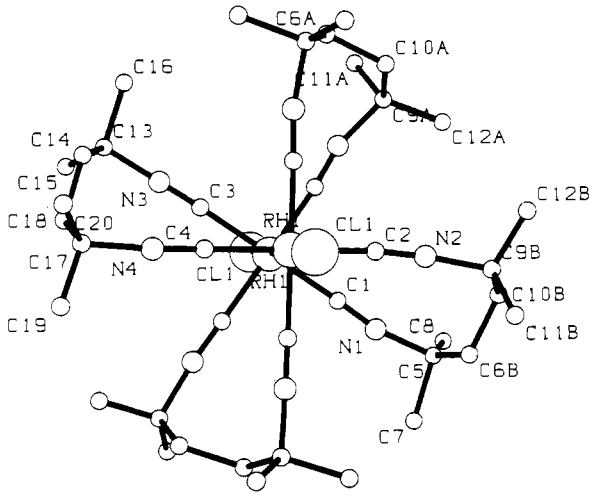

Figure 1. PLUTO[9c] drawing of the $Rh_2(TMB)_4Cl_2^{2+}$ cation, showing the numbering scheme and the conformation of the ligands. The angle ω (~33°) (C1–Rh1–Rh1′–C2, C3–Rh1–Rh1′–C4) can be seen, and CH_2–CH_2 bond vectors C6–C10 and C14–C18 are all approximately perpendicular to the metal–metal bond. The disordered atoms C6, C9, C10, C11, and C12 are shown in A and B sets, one in one TMB ligand and the other in the ligand related by the 2-fold axis, to show the similarity of their conformations.

Other Chemicals and Procedures. Deuteriated solvents for NMR spectra were obtained from Bio-Rad Laboratories and stored over activated molecular sieves, either directly (CD_2Cl_2) or following distillation from P_2O_5 (CD_3CN). Other materials were standard reagent or spectrophotometric grade and were used as supplied. Samples for NMR work were prepared in vacuum-sealed tubes, and ^1H NMR spectra were recorded on a JEOL FX-90Q instrument. The NMR spectra were recorded with CD_3CN as solvent to maximize the solubility of the complexes, except in the case of $Rh_2(TMB)_4^{2+}$, which was studied in CD_2Cl_2 because its coalescence temperature was too low for accurate measurement in CD_3CN.

Solution and Refinement of Structures. Data collection and refinement parameters appear in Table I.

For $[Rh_2(TMB)_4Cl_2](PF_6)_2$, diffraction symmetry and systematic absences indicated the space group *Pbcn*. The structure was solved by direct methods (SHELX76[9a]); Rh and Cl positions were used for initial phasing, and all other non-hydrogen atoms were located in subsequent Fourier syntheses. When anisotropic refinement of non-hydrogen atoms converged, the presence of some large thermal ellipsoids suggested disorder, especially in the TMB moiety at C(11) and C(12). Half-weight atoms were tested at C(6), C(9), C(10), C(11), and C(12), and these were separated into two sets: "A" and "B". Bond distances, bond angles, and isotropic temperature factors were constrained within each set; the occupancies (total fixed at 1.00) were refined and converged to about 0.41 (A) and 0.59 (B). The two sets have the same conformation; the positions are separated by 0.43 (C(6A)–C(6B)) to 1.00 Å (C(12A)–C(12B)). Displacement parameters suggest that the disorder may extend to other ligand atoms. The asymmetric unit contains half of the cation; since the occupancies are near 0.5, the disorder might be about the 2-fold axis (perpendicular to the Rh–Rh bond) that generates the other half, or it might be due to slightly different orientations of the cation in the crystal. The numbering scheme is shown in Figure 1, where the "A" set is shown at x, y, z and the "B" set in the $1.0 - x, y, 0.5 - z$ 2-fold-related position.

The data for $[Ir_2(TMB)_4I_2](BPh_4)_2$ were corrected for absorption (see Table I) and for decay during collection (ca. 4%). The space group from previous photographs and from measured intensities is *Pccn*. Ir and I atoms in this space group lie on a 2-fold axis parallel to z and thus make no contribution to reflections with odd l. A combination of direct methods (SHELX76[9a], with odd-l reflections upweighted), the Patterson map, and many Fourier syntheses was used to solve the structure. All non-H atoms were found. Rigid-body and constrained refinement with unconstrained isotropic displacement parameters was employed for C and N atoms; anisotropic displacement parameters were refined for Ir, I, and B; at convergence, the difference map showed peaks of about 3 e Å^{-3} along the I–Ir–Ir–I line and also showed peaks in two locations that resembled acetone molecules. Since the measured density (1.33 g mL^{-1}, by flotation) was greater than that calculated for $[Ir_2(TMB)_4I_2](BPh_4)_2$ (1.26 g mL^{-1}) and acetone had been the solvent used for recrystallization, acetone molecules were introduced as rigid bodies in the refinement with a total occupancy of 6 per unit cell or 1.5 per formula unit. This formulation leads to a calculated density of 1.32 g mL^{-1}.

The final difference map still shows peaks near the heavy atoms. Some strong reflections (especially [012] and [110]) show evidence of extinction. Some large displacement parameters (especially in the acetone and BPh_4^- moieties) and the severe anisotropy of the Ir atoms suggest disorder. On the other hand, the relatively small values of $\langle U^2 \rangle$ (ca. 0.08 Å^2) for the TMB C atoms suggest that the model is reasonable and the ligand conformation is correct.

Both structures were refined with SHELX76,[9a] scattering factors were taken from ref 9b, and calculations were performed on a DEC VAX 11/750 computer. Final coordinates appear in Tables II and III.

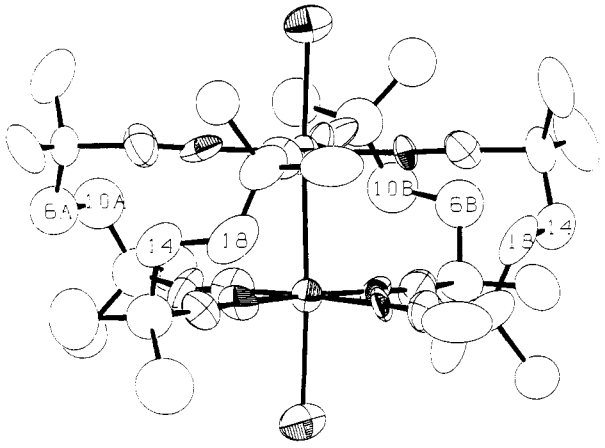

Figure 2. ORTEP[9d] drawing of the Rh cation. Ellipsoids are shown at 50% probability, and the disordered atoms are displayed as in Figure 1. Ligand $-CH_2-$ carbons are labeled.

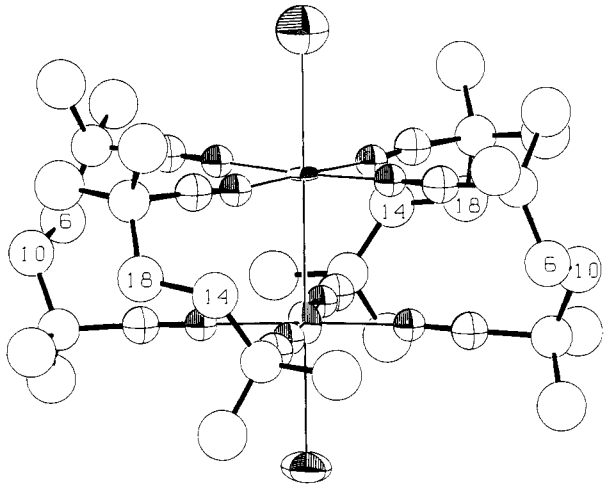

Figure 3. ORTEP[9d] drawing of the Ir cation. The numbering is similar to that in Figure 1, except that the 2-fold axis here is along the I–Ir–Ir–I axis. Ellipsoids for I and Ir are drawn at 50% probability; C and N atoms have been given average isotropic displacement parameters. Ligand $-CH_2-$ carbon atoms are labeled to clarify the conformation.

Results and Discussion

General Description of the Structures. Figure 1 (PLUTO[9c]) shows the geared disposition of the ligands, which is also emphasized in Figures 2 and 3, ORTEP[9d] drawings of the Rh and Ir complexes, respectively. (Completely numbered drawings are available as supplementary material.) Some distances and angles appear in Table V. The TMB bridges in the two complexes have the same

(9) (a) Sheldrick, G. M. "SHELX-76: A Program for Crystal Structure Determination"; Cambridge University Press: Cambridge, England, 1976. (b) *International Tables for X-ray Crystallography*; Kynoch: Birmingham, England, 1980; Vol. IV. (c) Motherwell, W. D. S.; Clegg, W. "PLUTO: Program for Plotting Molecular and Crystal Structures"; Cambridge University Press: Cambridge, England, 1978. (d) Johnson, C. K. "ORTEP-II: A Fortran Thermal-Ellipsoid Plot Program for Crystal Structure Illustrations"; Report No. ORNL-5138; National Technical Information Service, U.S. Department of Commerce: Springfield, VA, 1976.

Table II. Fractional Coordinates for $[Rh_2(TMB)_4Cl_2](PF_6)_2$[a]

atom	x	y	z
Rh	0.54064 (14)	0.48221 (7)	0.17577 (10)
Cl	0.6212 (5)	0.4820 (3)	0.0496 (3)
P	−0.0240 (8)	0.3096 (4)	−0.0347 (6)
F(1)	0.0003 (22)	0.3097 (10)	0.0538 (12)
F(2)	0.0871 (16)	0.3073 (11)	−0.0483 (19)
F(3)	−0.0460 (24)	0.3112 (9)	−0.1249 (11)
F(4)	−0.0096 (17)	0.2468 (7)	−0.0425 (13)
F(5)	−0.1303 (16)	0.3064 (15)	−0.0179 (21)
F(6)	−0.0226 (24)	0.3712 (8)	−0.0342 (15)
C(1)	0.4282 (18)	0.4433 (10)	0.1306 (12)
N(1)	0.3623 (16)	0.4221 (9)	0.1019 (13)
C(2)	0.4002 (20)	0.4134 (9)	0.3016 (13)
N(2)	0.3581 (18)	0.3745 (8)	0.2886 (10)
C(3)	0.6526 (16)	0.5209 (11)	0.2179 (13)
N(3)	0.7177 (16)	0.5440 (8)	0.2383 (12)
C(4)	0.5164 (14)	0.5516 (9)	0.3496 (12)
N(4)	0.5488 (16)	0.5932 (7)	0.3667 (11)
C(5)	0.2817 (19)	0.3837 (10)	0.0745 (13)
C(7)	0.2069 (19)	0.4290 (11)	0.0420 (18)
C(8)	0.3207 (22)	0.3563 (13)	0.0062 (16)
C(13)	0.8034 (22)	0.5752 (11)	0.2697 (17)
C(14)	0.7623 (21)	0.6028 (13)	0.3460 (14)
C(15)	0.8420 (22)	0.6107 (13)	0.2030 (18)
C(16)	0.8804 (23)	0.5298 (15)	0.2922 (20)
C(17)	0.6036 (27)	0.6463 (11)	0.3832 (16)
C(18)	0.6848 (22)	0.6459 (10)	0.3266 (18)
C(19)	0.5354 (26)	0.6881 (11)	0.3621 (16)
C(20)	0.6265 (21)	0.6497 (11)	0.4740 (13)
C(6A)	0.245 (2)	0.351 (3)	0.145 (2)
C(6B)	0.227 (2)	0.365 (2)	0.148 (1)
C(9A)	0.332 (5)	0.316 (1)	0.264 (1)
C(9B)	0.291 (2)	0.326 (1)	0.274 (1)
C(10A)	0.326 (5)	0.313 (1)	0.174 (1)
C(10B)	0.281 (3)	0.317 (1)	0.185 (1)
C(11A)	0.228 (5)	0.314 (5)	0.299 (3)
C(11B)	0.191 (2)	0.338 (2)	0.310 (2)
C(12A)	0.404 (7)	0.273 (3)	0.293 (3)
C(12B)	0.336 (4)	0.275 (1)	0.312 (2)

[a] Units of each esd, in parentheses, are those of the least significant digit of the parameter. Hydrogen atoms were either refined riding or refined as atoms in rigid groups. A and B designate disordered atoms; C–C and C–N distances and angles in this region were constrained. Final occupancy: 0.41 (A), 0.59 (B). A complete table of positional and displacement parameters is available as supplementary material.

conformation (within experimental error), in spite of quite different counterions and the presence of solvent in the Ir complex. Though each complex is chiral, the enantiomers are present in equal proportions in these centrosymmetric space groups. The conformation may be described by the torsion angles C–M–M–C (33° for Rh and 31° for Ir; see Figure 1 and Table V) and C–CH_2–CH_2–C (138° for Rh and 130° for Ir). The metal ion geometry is octahedral, with the longer axial (M–M and M–X) vectors oriented approximately (M = Rh) or exactly (M = Ir) along *c* in the crystals. The parallel equatorial planes of the interpenetrating octahedra are thus rotated with respect to each other, as in **I**.

NMR Studies in Solution. Binuclear complexes of "bridge" are expected to be relatively rigid, and the small ellipsoids of vibration observed in their crystal structures[7,10] support that expectation. In contrast, the larger ellipsoids and crystallographic disorder observed for the TMB complexes (ref 7 and this work) suggest considerably greater flexibility even in the solid state. Also, although the phosphorescence intensities and lifetimes for $Rh_2(bridge)_4^{2+}$ and $Rh_2(TMB)_4^{2+}$ are similar at low temperatures, those for $Rh_2(TMB)_4^{2+}$ are much reduced at room temperature.[11] Finally, this flexibility had been suggested as an explanation for the relatively large Stokes shift for fluorescence in $Rh_2(TMB)_4^{2+}$.[7] We were therefore interested in additional experimental data concerning the possibility of rotational isomerism.

The ^1H resonances due to methyl and methylene groups of TMB in $Rh_2(TMB)_4^{2+}$, $Rh_2(TMB)_4Br_2^{2+}$, $Ir_2(TMB)_4^{2+}$, and $Ir_2(TMB)_4I_2^{2+}$ are relatively simple at room temperature; the complexity expected from the solid-state conformations is not observed in NMR spectra until the samples are cooled. At lower temperatures the methyl resonances split and the methylene signals become more complicated. These results are presented graphically for $Rh_2(TMB)_4Br_2^{2+}$ in Figure 4. Spectra for the other complexes are similar; the major qualitative difference among them is the separation between the methyl and methylene resonances, which is greater for the oxidized (d^7) complexes. Chemical shift values and methyl group coalescence temperatures T_c for the four com-

Table III. Positional parameters for $[Ir_2(TMB)_4I_2](BPh_4)_2 \cdot 1.5(CH_3)_2CO$[a]

atom	x	y	z
Ir(1)	0.2500	0.2500	0.4442 (1)
Ir(2)	0.2500	0.2500	0.3268 (1)
I(3)	0.2500	0.2500	0.2128 (2)
I(4)	0.2500	0.2500	0.5578 (2)
C(1)	0.155 (2)	0.203 (1)	0.447 (2)
N(1)	0.097 (2)	0.176 (1)	0.448 (2)
C(2)	0.212 (2)	0.184 (1)	0.325 (2)
N(2)	0.174 (2)	0.147 (1)	0.323 (1)
C(3)	0.369 (1)	0.224 (1)	0.329 (1)
N(3)	0.438 (1)	0.205 (1)	0.327 (1)
C(4)	0.326 (3)	0.194 (1)	0.443 (2)
N(4)	0.369 (2)	0.160 (1)	0.448 (1)
C(5)	0.037 (2)	0.132 (1)	0.450 (1)
C(6)	0.020 (3)	0.114 (1)	0.391 (2)
C(7)	−0.046 (3)	0.158 (2)	0.473 (2)
C(8)	0.070 (3)	0.108 (2)	0.504 (2)
C(9)	0.141 (3)	0.096 (1)	0.318 (2)
C(10)	0.099 (3)	0.082 (2)	0.375 (2)
C(11)	0.227 (3)	0.066 (1)	0.312 (2)
C(12)	0.072 (3)	0.098 (2)	0.272 (2)
C(13)	0.532 (1)	0.185 (1)	0.331 (2)
C(14)	0.528 (4)	0.154 (2)	0.384 (2)
C(15)	0.594 (3)	0.227 (1)	0.325 (2)
C(16)	0.545 (3)	0.156 (1)	0.277 (1)
C(17)	0.414 (2)	0.111 (1)	0.449 (2)
C(18)	0.466 (3)	0.111 (2)	0.393 (2)
C(19)	0.343 (3)	0.072 (1)	0.455 (2)
C(20)	0.481 (3)	0.112 (2)	0.497 (2)
B	0.7420 (11)	0.0221 (6)	0.3779 (6)
C(21)	0.634 (1)	0.013 (1)	0.368 (1)
C(27)	0.774 (1)	0.069 (1)	0.339 (1)
C(33)	0.762 (2)	0.033 (1)	0.446 (1)
C(39)	0.799 (2)	−0.026 (1)	0.358 (1)
CAC(2)	0.982 (4)	0.228 (2)	0.119 (2)
OAC(1)	0.943 (5)	0.226 (2)	0.074 (3)
CAC(1)	1.027 (4)	0.182 (2)	0.141 (3)
CAC(3)	0.997 (5)	0.276 (2)	0.148 (3)
OAC(2)	0.750	0.250	0.476 (4)
CAC(4)	0.750	0.250	0.527 (4)
CAC(5)	0.730 (14)	0.204 (2)	0.560 (4)

[a] BPh_4^- phenyl groups and acetone molecules were refined as rigid groups; distances and some angles for all C and N atoms shown here were constrained. H atoms in the ligand were riding or were included in rigid groups. A complete table of positional and displacement parameters is available as supplementary material.

Table IV. Data from ^1H NMR Spectra for Rh and Ir Complexes of TMB

complex	chem shift[a] $-CH_2-$ (fast)	$-CH_3$ (fast)	$-CH_3$ (slow)	T_c/ °C	ΔG^*/ kJ mol^{-1}
$Rh_2(TMB)_4^{2+}$[b]	1.90	1.54	1.34, 1.58	−32	50.8
$Rh_2(TMB)_4Br_2^{2+}$[c]	2.16	1.58	1.42, 1.63	−11	55.7
$Ir_2(TMB)_4^{2+}$[c]	1.72	1.46	1.33, 1.58	15	61.1
$Ir_2(TMB)_4I_2^{2+}$[c]	2.11	1.54	1.33, 1.63	−14	54.3

[a] Given as δ vs. TMS. "Fast" and "slow" refer to values determined in the fast-exchange and stopped-exchange limits, respectively. [b] In CD_2Cl_2. [c] In CD_3CN.

(10) Mann, K. R.; Bell, R. A.; Gray, H. B. *Inorg. Chem.* **1979**, *18*, 2671.
(11) Rice, S. F.; Milder, S. J.; Gray, H. B.; Goldbeck, R. A.; Kliger, D. S. *Coord. Chem. Rev.* **1982**, *43*, 349.

Table V. Geometric Parameters for Polynuclear Isocyanide Complexes[a]

complex[b]	M–M/Å	ω/deg	M–M–C/deg	M–C–N/deg	ref
$Rh_2(bridge)_4^{2+}$	3.24	0	88–89	175–176	7
$Rh_2(TMB)_4^{2+}$	3.26	23, 28	91–93	175	7
$Rh_2(DMB)_4^{2+}$	4.48	0	85–95	174–180	27
$Rh_2(CNPh)_8^{2+}$	3.19	39, 42	87–103	173–178	2
$Rh_2(CNC_6H_4\text{-}p\text{-}F)_8^{2+}$	3.29	2	81–103	173–178	23
$Rh_2(t\text{-}Bu\text{-}DiNC)_4^{2+}$	3.38	2	67–121	173–177	24
$Rh_3(CNCH_2Ph)_{12}I_2^{3+}$	2.80	40, 50	89–96	175–179	26
$Rh_4(bridge)_8Cl^{5+}$	2.93, 2.92[c] 2.77[d]	0, 12[c] 45[d]	87–92	173–177	22
$Rh_2(bridge)_4Cl_2^{2+}$	2.84	0	90	178	10
$Rh_2(TMB)_4Cl_2^{2+}$	2.77	33	89–92	175–178	e
$Ir_2(TMB)_4I_2^{2+}$	2.80	31	88–92	167–178	e
$Rh_2(TMB)_4(Mn(CO)_5)_2^{2+}$	2.92	25	88–92	170–178	13
$Rh_2(CNC_6H_4\text{-}p\text{-}CH_3)_8I_2^{2+}$	2.79	28–35	89–92	172–177	25
$Co_2(CNCH_3)_{10}^{4+}$	2.74	43–51	86–89	171–178	17
$Ru_2(CNXyl)_{10}^{2+}$	3.00	0, 6	84–97	169–175	21b

[a] Angles and distances are rounded to 1° and 0.01 Å, respectively. Multiple values, or lower and upper limits, are given where appropriate. [b] The six d^8 complexes are listed first, followed by the two intermediate-oxidation-state (d^7/d^8) and the seven d^7 complexes. Weakly bound axial ligands are omitted from the Rh(I) formulas for simplicity. See text for ligand abbreviations. [c] Within the two Rh_2 units. [d] Between the two Rh_2 units. [e] This work.

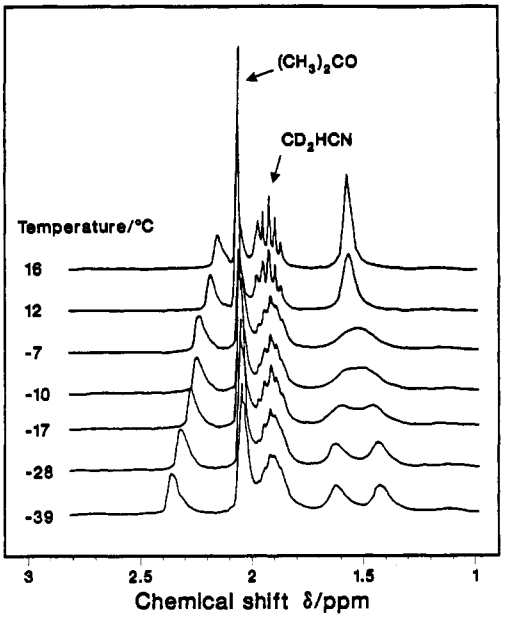

Figure 4. Variable-temperature ^1H NMR spectra (90 MHz) for $Rh_2(TMB)_4Br_2^{2+}$ in CD_3CN, showing changes in methyl (δ 1.58) and methylene (δ 2.16 at 16 °C) resonances. The acetone resonance (δ 2.05) is due to acetone of crystallization in the $Rh_2(TMB)_4Br_2^{2+}$ salt.

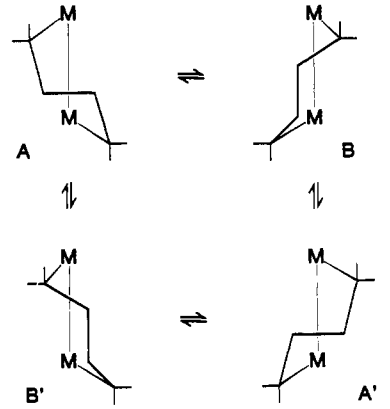

Figure 5. Scheme for interconversion of rotational isomers of $M_2(TMB)_4$ complexes, with one TMB ligand shown in each case for simplicity. Crystal structure data (this work and ref 7 and 13) suggest that the A isomer and its enantiomer A′ are lowest in energy. Complete racemization of the complex (A ⇄ A′) according to this scheme would require a rotation about the metal–metal axis (A ⇄ B or B′ ⇄ A′) and a "methylene twist" (A ⇄ B′ or B ⇄ A′).

plexes studied are given in Table IV.

The most attractive explanation for these dynamic NMR observations is that the chiral structure seen in the solid state persists in solution only at low temperatures, racemization occurring more rapidly as the temperature is increased. Calculated free energies of activation for the process are given in Table IV.[12]

A plausible scheme for the racemization process is illustrated in Figure 5. In the figure the M—C≡N—C linkages are assumed to be linear, giving the entire complex the appearance of a set of interlocked six-membered rings. The conformations in the figure then correspond approximately to the familiar "chair" and "skew-boat" forms of cyclohexane. (The "skew-boat" conformation is found in the two structures reported here, as well as in the two TMB-complex structures previously described.[7,13]) Because it involves relatively little change in the bond and torsion angles within the TMB ligands, rotation about the metal–metal axis (A ⇄ B and A′ ⇄ B′ in Figure 5) probably involves a smaller activation barrier than the "methylene twist", which connects A with B′ and B with A′.

Based on our dynamic NMR data, the rate constant for racemization of $Rh_2(TMB)_4^{2+}$ is ca. 2×10^4 s^{-1} in CH_3CN at 25 °C. This rate constant is too small to account directly for the observed room-temperature $^3A_{2u}$ lifetime of 25 ns.[11] However, a smaller barrier, such as that proposed for the A ⇄ B and A′ ⇄ B′ metal–metal rotations in Figure 5, would lead to a significantly larger rate constant. A more recent photophysical study of the excited-state decay also found activation energies substantially smaller than the present NMR-derived values.[14] We therefore propose that partial rotation about the metal–metal axis, and the associated small changes in Rh–Rh distance, may be sufficient to cause deactivation of the $^3A_{2u}$ excited state of $Rh_2(TMB)_4^{2+}$.

(12) The equation $\Delta G^{\ddagger} = -RT_c \ln (h\pi\Delta\nu/(2^{1/2}k_BT_c))$ was used, based on the approximation $\pi(\Delta\nu)/2^{1/2}$ for the coalescence rate constant k_c (Pople, J. A.; Schneider, W. G.; Bernstein, H. J. *High-Resolution Nuclear Magnetic Resonance*; McGraw-Hill: New York, 1959; p 223) and the Eyring equation $\Delta G^{\ddagger} = -RT \ln (\kappa hk/(k_BT))$ (Glasstone, S.; Laidler, K. J.; Eyring, H. *The Theory of Rate Processes*; McGraw-Hill: New York, 1941; p 195), assuming unit transmission coefficient κ. In a separate experiment employing a Bruker 500-MHz instrument, coalescence for the $Rh_2(TMB)_4^{2+}$ methyl resonances was observed at −19 °C. On the basis of the value of $\Delta G^{\ddagger}$ calculated for this experiment (50.1 kJ mol^{-1}), we estimate that the activation parameters $\Delta H^{\ddagger}$ and $\Delta S^{\ddagger}$ for $Rh_2(TMB)_4^{2+}$ are ca. 64 kJ mol^{-1} and 54 J mol^{-1} K^{-1}, respectively.

(13) Bohling, D. A.; Gill, T. P.; Mann, K. R. *Inorg. Chem.* **1981**, *20*, 194.
(14) Milder, S. J. *Inorg. Chem.* **1985**, *24*, 3376.

Two other aspects of the excited-state decay are of importance. First, the metal–metal interactions in the d^8 $^3A_{2u}$ excited states are similar to those in the ground states of the corresponding d^7 species. The similarity of the NMR data for the d^7 and d^8 complexes therefore suggests that dynamic processes are comparable in the d^8 ground and excited states. And second, in contrast to the behavior of $Rh_2(TMB)_4^{2+}$, the $^3A_{2u}$ lifetime for $Ir_2(TMB)_4^{2+}$ is approximately the same (ca. 200 ns) at both room temperature and 77 K.[15] Thus, rotation of the type observed in the NMR spectra probably contributes substantially to excited-state decay only for the Rh(I) complex. It has been proposed[3] that decay of rhodium(I) isocyanide complex excited states involves intermediate d–d states. Such states would be considerably higher in energy in Ir(I), and this would mean that rotation about the metal–metal axis might not cause deactivation of $^3A_{2u}$ in $Ir_2(TMB)_4^{2+}$. However, other decay mechanisms may also be consistent with the observed photophysical data.[14] A more detailed study of the photophysics of iridium(I) species with a variety of diisocyanide ligands is likely to be of use in rationalizing the excited-state nonradiative decay rates.

Comparison with Other Structures. The general M_2L_8 structure **1** of D_4 symmetry (D_{4d} and D_{4h} symmetries occur for the special cases of $\omega = 45°$ and $\omega = 0°$, respectively) is known for a large number of metal complexes. In the great majority of these complexes the two metal atoms are joined by a formal single or multiple bond. The two major geometrical features of this structure that have been examined most often are the separation between the ML_4 moieties and the torsion angle ω. In simple M_2L_8 complexes, the presence of the eclipsed conformation, which is expected to cause substantial steric repulsion between ligands, can frequently be attributed to electronic factors.[16] Polyatomic ligands L (including CO as well as isocyanides) offer additional degrees of freedom by which steric and electronic contributions to molecular geometry can be compared. Finally, bridging bidentate ligands provide connectivity constraints on the various distances and on ω. Our goal was to compare the structures reported above to those of other polynuclear isocyanide complexes in the literature, in order to evaluate the importance of these steric and electronic effects.

The high symmetry of the metal σ- and π-type orbitals suggests that, for formal metal–metal bond orders of 0, 1, or 3, there will be no electronic preference for specific values of ω. Under these conditions steric factors should favor torsion angles near 45°. This agrees with the results of early studies of the singly bonded $Mn_2(CO)_{10}$[17] and $Co_2(CNCH_3)_{10}^{2+}$[18] and with more recent examinations of complexes such as $(R_3P)(CO)_4Os$–$W(CO)_5$[19] and $Mn_3(CO)_{14}^-$.[20] There are, however, at least two exceptions: $((CH_3)_3Sn)(OC)_4Ru$–$Ru(CO)_4)(Sn(CH_3)_3)$[21a] and the isoelectronic $Ru_2(CNXyl)_{10}^{2+}$ (CNXyl = 2,6-dimethylphenyl isocyanide)[21b] adopt the eclipsed conformation in the solid state. These latter examples suggest that, at the metal–metal distances that are typical for these complexes (2.7–3.0 Å), energy differences between eclipsed and staggered conformations are small.

We were interested in the effects of bridging diisocyanide ligands not only on metal–metal distance and ω but also on the planarity of the $M(CNC)_4$ unit. In complexes in which the electronically and sterically ideal metal–metal distances are similar, the environment around the metal atoms should be essentially planar. Results from these and other crystallographic studies are presented in Table V.

Initial reports of the crystal structures of the Rh(I)[7] and Rh(II)[10] complexes of "bridge" allowed a comparison of bond distances and angles. Both complexes are eclipsed ($\omega = 0°$), and the complex of Rh(II) shows the smaller deviations from ideal Rh–Rh–C (90°) and Rh–C–N (180°) angles. This seems reasonable, since the metal–metal distance in the Rh(II) complex is considerably closer to the "bite" distance for a three-carbon bridging group (ca. 2.5 Å). In the tetranuclear ion $Rh_4(bridge)_8Cl^{5+}$,[22] the central Rh_4^{6+} core has an overall formal metal–metal bond order of 1. Here the results are similar to those for $Rh_2(bridge)_4^{2+}$, except that, because the bridged Rh–Rh distance is shorter in the tetranuclear complex, the deviation from ideal angles is smaller. (This structure is also of interest in that one of its $Rh_2(bridge)_4$ moieties shows a nonzero torsion angle ω.)

The geometry of $Rh_2(TMB)_4^{2+}$[7] also shows little deviation from ideal angles, suggesting that the presence of a fourth carbon atom in the bridging group is more appropriate for the characteristic Rh(I)–Rh(I) separation. Similar results were observed for the formally Rh(II) complex $Rh_2(TMB)_4(Mn(CO)_5)_2^{2+}$,[13] in which the metal–metal distance is significantly longer than that found for the other Rh(II) and Ir(II) complexes. The present study of $Rh_2(TMB)_4Cl_2^{2+}$ and $Ir_2(TMB)_4I_2^{2+}$, on the other hand, shows a slight compression of the metal atoms relative to the bridging ligands: for example, in both complexes the metal atoms are ca. 0.15 Å closer together than the planes formed by the isocyanide N atoms.

Our data, and data from other structural studies in the literature, enable us to evaluate the relative importance of metal–metal electronic interactions and intraligand conformational energy in determining the amount and distribution of strain within the metal complexes. Although the complexes of bridging diisocyanides show strong regularities, as outlined above, the data for the seven unbridged species (see Table V) are much less consistent. The binuclear rhodium(I) complexes of phenyl isocyanide[3] and *p*-fluorophenyl isocyanide[23] show reasonable Rh–Rh distances but vary widely in the other tabulated parameters. One of the ligands in $Rh_2(CNPh)_8^{2+}$ is bent substantially out of the $Rh(CN)_4$ plane, for example, and the metal–metal vector in $Rh_2(CNC_6H_4$-*p*-$F)_8^{2+}$ makes an angle of only ca. 80° with the RhL_4 planes. The rhodium(I) complex $Rh_2(t$-Bu-DiNC$)_4^{2+}$, in which *t*-Bu-DiNC is the chelating diisocyanide

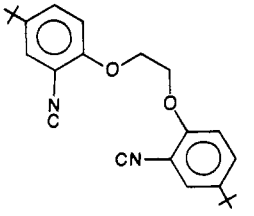

has recently been prepared by Angelici and co-workers.[24] This

(15) Smith, T. P. Ph.D. Thesis, California Institute of Technology, 1982.
(16) One example is the influence of the δ component of metal–metal quadruple bonds. For studies of steric influences on ω in triply and quadruply bonded systems, see: (a) Hopkins, M. D.; Zietlow, T. C.; Miskowski, V. M.; Gray, H. B. *J. Am. Chem. Soc.* **1985**, *107*, 510. (b) Carroll, T. L.; Shapley, J. R.; Drickamer, H. G. *J. Am. Chem. Soc.* **1985**, *107*, 5802. (c) Peacock, R. D.; Fraser, I. F. *Inorg. Chem.* **1985**, *24*, 988. (d) Bursten, B. E.; Cotton, F. A.; Fanwick, P. E.; Stanley, G. G.; Walton, R. A. *J. Am. Chem. Soc.* **1983**, *105*, 2606. (e) Cotton, F. A.; Stanley, G. G.; Walton, R. A. *Inorg. Chem.* **1978**, *17*, 2099. (f) Cotton, F. A.; Fanwick, P. E.; Fitch, J. W.; Glicksman, H. D.; Walton, R. A. *J. Am. Chem. Soc.* **1979**, *101*, 1752.
(17) Dahl, L. F.; Rundle, R. E. *Acta Crystallogr.* **1963**, *16*, 419.
(18) Cotton, F. A.; Dunne, T. G.; Wood, J. S. *Inorg. Chem.* **1964**, *3*, 1495.
(19) Einstein, F. W. B.; Jones, T.; Pomeroy, R. K.; Rushman, P. *J. Am. Chem. Soc.* **1984**, *106*, 2707.
(20) Bau, R.; Kirtley, S. W.; Sorrell, T. N.; Winarko, S. *J. Am. Chem. Soc.* **1974**, *96*, 988.
(21) (a) Howard, J. A. K.; Kellett, S. C.; Woodward, P. *J. Chem. Soc., Dalton Trans.* **1975**, 2332. (b) Chalmers, A. A.; Liles, D. C.; Meintjies, E.; Oosthuizen, H. E.; Pretorius, J. A.; Singleton, E. *J. Chem. Soc., Chem. Commun.* **1985**, 1340. That steric repulsions among the bulky XylNC ligands in this structure play an important role in determining the conformation is supported by the unusually large Ru–Ru distance (3.00 Å; see Table V).
(22) Mann, K. R.; DiPierro, M. J.; Gill, T. P. *J. Am. Chem. Soc.* **1980**, *102*, 3965.
(23) Endres, H.; Gottstein, N.; Keller, H. J.; Martin, R.; Rodemer, W.; Steiger, W. *Z. Naturforsch., B: Anorg. Chem., Org. Chem.* **1979**, *34B*, 827. The Rh–Rh distance given in Table II for $Rh_2(CNC_6H_4$-*p*-$F)_8^{2+}$ (3.29 Å), calculated from the coordinates and cell dimensions of Endres and co-workers, differs slightly from that (3.21 Å) reported in the paper; we thank the editors of the Cambridge Crystallographic Data File for discovering this apparent error.
(24) Plumner, P. T.; Karcher, B. A.; Jacobson, R. A.; Angelici, R. J. *J. Organomet. Chem.* **1984**, *260*, 347.

complex adopts a "slipped-stacked" structure, similar to that of $Rh_2(CNC_6H_4$-p-$F)_8^{2+}$,[23] with a 67° angle between the Rh–Rh vector and the $Rh(CN)_4$ planes.

In the d^7 and mixed-valence systems $Co_2(CNCH_3)_{10}^{4+}$,[17] $Ru_2(CNXyl)_{10}^{2+}$,[21b] $Rh_2(CNC_6H_4$-p-$CH_3)_8I_2^{2+}$,[25] and $Rh_3(CNCH_2Ph)_{12}I_2^{3+}$,[26] the structures are somewhat more regular than those of the d^8 species. However, substantial variations exist even among these oxidized complexes.

Another bridged structure in the literature sheds light on the strength of the electronic forces between the metal atoms in these complexes. In $Rh_2(DMB)_4^{2+}$,[27] the large rigid ligands are able to force the metal atoms much farther apart than they are in the other bridged and unbridged d^8 complexes. In this case, therefore, the steric constraints due to the DMB ligand appear to have overwhelmed any electronic preference for a particular Rh–Rh distance or torsion angle ω.

Summary

The crystal structures of two new d^7–d^7 systems involving the bridging ligand TMB, including the first structure reported for a binuclear Ir(II) isocyanide complex, have been determined and compared with those of other polynuclear isocyanide complexes. Data from NMR experiments show that TMB complexes have substantial conformational mobility; this mobility may be responsible for the unusually rapid deactivation of the $^3A_{2u}$ excited state in $Rh_2(TMB)_4^{2+}$.

Detailed crystallographic comparisons suggest that the bridging ligands enforce a geometrical regularity not present in the unbridged structures. The following conclusions can be drawn. While the relatively compact "bridge" ligand suffers less distortion in its Rh(II) complex than in the Rh(I) complex, the opposite is true of TMB. Torsion angles ω tend to be larger in Rh(II) and Ir(II) structures than in those of Rh(I). Also, the wide variety among the unbridged structures suggests that packing forces, either among the ligands or between the ligands and counterions, can easily surpass the electronic forces associated with bending bonds to the metal atom. Thus, the geometric preferences of the metal atoms appear to be limited to the bond length, and the steric requirements of the ligands (perhaps including the crystal packing, in the case of nonbridging ligands) appear to control the angle ω.

Acknowledgment. We thank Professor Jack D. Dunitz for making his diffractometer available for data collection on $[Rh_2(TMB)_4Cl_2](PF_6)_2$. We thank Professor Dunitz, Paul Seiler, and Dr. Richard E. Marsh for numerous helpful discussions. Johnson Matthey Inc. is acknowledged for a generous loan of rhodium and iridium compounds. This research was supported by the National Science Foundation.

Registry No. $[Ir_2(TMB)_4](BPh_4)_2$, 110904-71-7; $[Ir_2(TMB)_4I_2](BPh_4)_2$, 99327-03-4; $[Ir_2(TMB)_4I_2](BPh_4)_2 \cdot x(CH_3)_2CO$, 110904-69-3; $[Rh_2(TMB)_4](BPh_4)_2$, 110904-67-1; $[Rh_2(TMB)_4Br_2](BPh_4)_2$, 99326-95-1; $[Rh_2(TMB)_4Cl_2](PF_6)_2$, 99326-92-8; Rh, 7440-16-6; Ir, 7439-88-5.

Supplementary Material Available: Fully labeled ORTEP[9d] drawings for $Rh_2(TMB)_4Cl_2^{2+}$ and $Ir_2(TMB)_4I_2^{2+}$ and tables of positional and displacement parameters, bond distances, bond angles, and torsion angles (12 pages); tables of observed and calculated structure factors (21 pages). Ordering information is given on any current masthead page.

(25) Olmstead, M. M.; Balch, A. L. *J. Organomet. Chem.* **1978**, *148*, C15–C18. We thank Professor Balch for providing us with the atomic coordinates for this structure and the structure in ref 26.
(26) Balch, A. L.; Olmstead, M. M. *J. Am. Chem. Soc.* **1979**, *101*, 3128.
(27) Mann, K. R. *Cryst. Struct. Commun.* **1981**, *10*, 451.

Contribution from the Department of Chemistry, University of New Mexico, Albuquerque, New Mexico 87131

Reactions of Tris(trimethylsilyl)aluminum and Ammonia. Formation, Structure, and Thermal Decomposition of $[(Me_3Si)_2AlNH_2]_2$

J. F. Janik, E. N. Duesler, and R. T. Paine*

Received June 25, 1987

The reaction of $(Me_3Si)_3Al \cdot Et_2O$ and NH_3 in a 1:1 ratio results in the formation of $[(Me_3Si)_2AlNH_2]_2$. The compound has been characterized by elemental analysis, mass, infrared, and NMR spectroscopic data, and single-crystal X-ray diffraction analysis. The compound crystallizes in the monoclinic space group $P2_1/n$ with a = 9.364 (1) Å, b = 8.171 (2) Å, c = 16.781 (3) Å, β = 95.78 (1)°, Z = 2, V = 1277.4 (4) Å^3, and ρ = 0.98 g cm^{-3}. Least-squares refinement gave R_F = 4.15% and R_{wF} = 3.85% on 2068 independent reflections with $F \geq 4\sigma(F)$. The molecule contains a central planar four-membered Al–N–Al′–N′ ring with Al(1)–N(1) = 1.953 (2) Å, Al(1)–N(1′) = 1.956 (2) Å, Al(1)–N(1)–Al(1′) = 93.1 (1)°, and N(1)–Al(1)–N(1′) = 86.9 (1)°. Thermolysis of the dimer or a polymeric product, obtained from reactions of $(Me_3Si)_3Al \cdot Et_2O$ and excess ammonia, gives solid solutions of AlN and SiC.

Introduction

The coordination chemistry for alanes and tertiary amines has been extensively studied, and a large number of simple, stable acid–base complexes, $X_3Al \cdot NR_3$, have been isolated.[1] Alanes and NH_3, primary amines, and secondary amines also form a large number of adducts; however, these combinations show a pronounced tendency to undergo elimination–condensation reactions, which produce amino- and imino-substituted alanes.[1] The elimination reactions appear to be dependent upon aluminum–substituent group bond strengths, showing increasing ease of elimination from the aluminum fragment in the following order: Al–Cl < Al–R < Al–H.[1] Reaction temperatures in the combinations shown in eq 1–4 provide qualitative evidence for part of this series.[1-3] Although kinetic studies for these reaction systems are limited, it has been suggested that the elimination process is not preceded by, but instead may compete with, adduct formation. In fact, formation of an adduct may result in a "dead-end" state for elimination reactions.[4]

$$Et_2AlH + NH_3 \xrightarrow{0\ ^\circ C} (Et_2AlNH_2)_x + H_2 \quad (1)$$

$$Et_3Al + NH_3 \xrightarrow{25\ ^\circ C} (Et_2AlNH_2)_x + C_2H_6 \quad (2)$$

$$Et_2AlCl + NH_3 \xrightarrow{65\ ^\circ C} (Et(Cl)AlNH_2)_x + C_2H_6 \quad (3)$$

$$EtAlCl_2 + NH_3 \xrightarrow{128\ ^\circ C} (Cl_2AlNH_2)_x + C_2H_6 \quad (4)$$

(1) Mole, T.; Jeffery, E. A. *Organoaluminum Chemistry*; Elsevier: New York, 1972.
(2) Cohen, M.; Gilbert, J. K.; Smith, J. D. *J. Chem. Soc.* **1965**, 1092.
(3) Gilbert, J. K.; Smith, J. D. *J. Chem. Soc. A* **1968**, 233.
(4) Beachley, O. T.; Tessier-Youngs, C. *Inorg. Chem.* **1979**, *18*, 3188.

0020-1669/87/1326-4341$01.50/0